RESEARCH ARTICLE | DECEMBER 10 2025

Ambient-dependent reversal of unidirectional light scattering by metal–dielectric hybrid plasmonic nanoantenna

Shuto Watanabe ; Ryuichi Ohta ; Tsukasa Katayama ; Yoshito Y. Tanaka

APL Photonics 10, 126114 (2025)
https://doi.org/10.1063/5.0297764

APL Photonics ARTICLE pubs.aip.org/aip/app

Ambient-dependent reversal of unidirectional light scattering by metal–dielectric hybrid plasmonic nanoantenna

Cite as: APL Photon. 10, 126114 (2025); doi: 10.1063/5.0297764
Submitted: 21 August 2025 • Accepted: 24 November 2025 •
Published Online: 10 December 2025

Shuto Watanabe, Ryuichi Ohta,[a)] Tsukasa Katayama, and Yoshito Y. Tanaka[a)]

AFFILIATIONS

Research Institute for Electronic Science, Hokkaido University, Kita 21, Nishi 10, Kita-ku, Sapporo 001-0021, Hokkaido, Japan

[a)]**Authors to whom correspondence should be addressed:** ryuichi.ohta@es.hokudai.ac.jp and ytanaka@es.hokudai.ac.jp

ABSTRACT

Unidirectional light scattering of plasmonic nanoantennas extends toward various nanophotonic applications, such as optical routers, molecular sensors, and light-driven actuators. The controllability of the direction of scattered light is crucial for those applications. So far, the large controllability enabling the reversal of the scattering direction has been achieved by tuning the wavelength and polarization of the incident light. Asymmetric dielectric nanostructures can also induce either unidirectional or bidirectional light scattering. However, such control methods relying on the incident light parameters and previous architecture limit the practical applicability of unidirectional light scattering, especially in sensing applications. Here, we propose and demonstrate a new hybrid architecture to control and reverse the unidirectional light scattering with respect to the ambient conditions through the integration of paired gold plasmonic nanorods and asymmetric dielectric shield. The dielectric shields selectively make certain nanorod less influential to the surrounding refractive index change, which results in the substantial controllability of direction of the scattered light with respect to the surrounding medium. Fourier imaging of the scattered light experimentally reveals the reversal of the scattering direction over a broad wavelength range. Numerical simulations reproduce the spectral response and directional scattering for various surrounding media, demonstrating a wide dynamic range and high sensitivity for the ambient refractive indices. These findings suggest that the nanoantenna can detect local molecular adsorption, leading to a compact and tunable platform for ambient-dependent optical devices with potential applications in nanophotonic sensing, reconfigurable photonics, and environment-adaptive light-driven nanomotors.

I. INTRODUCTION

Metal nanoparticles exhibit localized surface plasmon resonances, which substantially enhance the light–matter interaction between incident photons and electrons in metals, even in subwavelength spatial regions. This strong field localization overcomes the spatial mismatches in photons and nanoscale materials and enables us to pave the way for notable applications, especially in high-resolution sensing, imaging, and spectroscopy along with the engineering of chemical reactions.[1–5] Furthermore, the local optical resonances modify the phases of scattered light and radiative photons, making them to be unidirectional as an optical analog to Yagi-antenna.[6–14] Directional light scattering has also been demonstrated using asymmetric and high-refractive-index dielectric nanostructures.[15–17] The unidirectional light scattering of nanoantennas extends various nanophotonic applications, including optical routers,[18–20] molecular sensors,[7,21,22] and light-driven actuators.[23–25]

The directionality of the nanoantennas arises from the phase differences between adjacent plasmonic oscillators and their spatial retardation. Therefore, the tuning of their relative phase provides the controllability of the direction of the light scattering in lateral. So far, the reversal and dynamic control of unidirectional light scattering have been demonstrated with antisymmetric plasmonic materials and geometries.[18,21,25–27] Owing to the symmetry-broken resonance pairs in the frequency and spatial domains, the relative phases and the direction have been controlled by the wavelength and polarization of the incident light.

Molecular adsorption onto the plasmonic nanoantennas significantly shifts the resonance frequency, which originates from the strong interaction between molecules and nanoantennas.[1,3,28,29] The strong field enhancement allows the highly sensitive detection of molecules at the single-molecule level.[3] This frequency shift modifies the directionality of the light scattering,[7,21] in which the directionality depends not only on the incident light but also on the ambient conditions. Due to the susceptibility of the plasmonic resonances to the adjacent environment and the phase sensitive scattering mechanism, this ambient-dependent unidirectional light scattering holds great potential for sensing applications with very small footprints. To obtain higher sensitivity and wider dynamic range in this scheme, the amount of phase shift is crucially important. However, the reported approach relying on the asymmetric catalytic reaction of palladium and gold antenna is inherently limited due to the broad linewidth, weak oscillator strength, and far detuned plasmonic resonance of palladium.[21,30] The steep spectral edges of Fano resonances in the nanoantenna can enhance the absolute phase shifts induced by molecular adsorption,[31,32] but the narrow bandwidth of such sharp resonances limits the operational wavelength range. Small controllability of unidirectional light scattering constrains the sensing applications and moreover hinders the broad expansion toward exotic nanophotonic devices and light-driven nanomotors.

In this paper, we demonstrate universal architecture for ambient-dependent unidirectional light scattering using paired gold nanorods and antisymmetric dielectric shields. Because of the geometric separation between the two nanorods, the dielectric shields selectively make certain nanorods less influential to the ambient condition while retaining their narrow linewidths and fine tunability of the initial detuning. It results in substantial phase differences between the paired nanorods with respect to the surrounding medium. In fact, we, for the first time, observed the reversal of unidirectional light scattering by changing the ambient environment from air to water. The maximum change in intensity ratio exceeded a factor of eight representing the high sensitivity and wide dynamic range using this architecture. The reversal wavelength of the incident light was exhibited over the spectral range of the gold nanorods. The measured light scattering patterns agreed with our numerical analyses and spectra in experiments. This metal–dielectric hybrid nanoantenna enables unidirectional light scattering depending on the density and temperature of the surrounding gas and solvent, which leads to the ambient-dependent self-regulating light-driven actuators.

II. RESULTS

Figure 1(a) schematically shows the optical responses and unidirectional light scattering from the plasmonic nanoantennas in this study. The nanoantennas consist of paired gold nanorods arranged laterally, with distinct geometries designed to support two optical resonances at different frequencies. The total scattered light of the nanoantenna is the sum of the scattering contributions from the two nanorods. By designing the lateral separation of the paired nanorods to induce a phase retardance of $\pi/2$, constructive interference is achieved on one side and destructive interference on the opposite side, resulting in unidirectional side scattering. The intensity ratio of laterally scattered light in the two opposing directions is maximized when the frequency of the incident light is tuned to the midpoint between the two resonances.

The resonance wavelengths of the plasmonic nanoantennas are inherently highly sensitive to the surrounding medium, including ambient gases and solvents. For instance, if water is applied, the two resonances move to longer wavelength due to the increase in

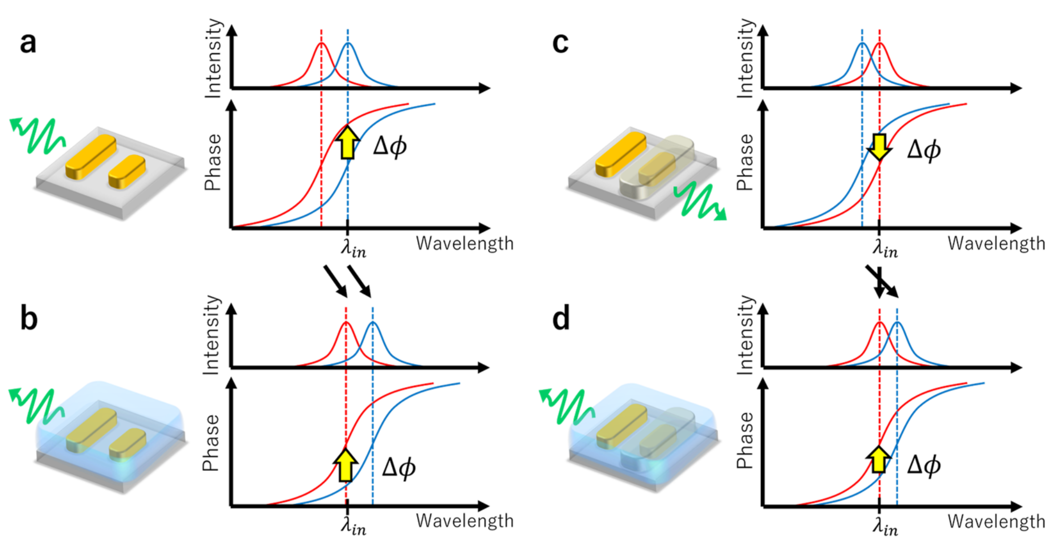

FIG. 1. Schematic images of the optical responses and unidirectional light scattering of a plasmonic nanoantenna in air (a) and water (b), and of a nanoantenna with an asymmetric dielectric shield in air (c) and water (d). The red (blue) curves represent the intensities and phases of the scattered light from the shorter (longer) nanorods. λ_{in} and $\Delta\phi$ indicate the incident laser wavelengths and relative phases of the scattered light from the two nanorods, respectively.

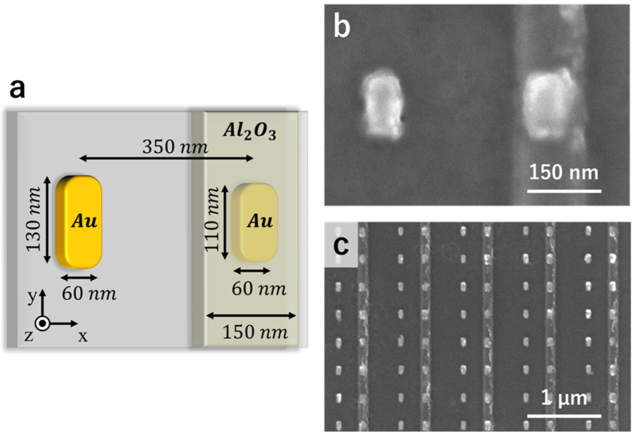

FIG. 2. Schematic (a) and SEM (b) images of the nanoantenna with the asymmetric dielectric shield. (c) A SEM image of the arrayed nanoantennas.

surrounding refractive index, as shown in Fig. 1(b). In this case, optimal wavelength for directional light scattering shifts accordingly, but the overall scattering direction does not change. In contrast, introducing an asymmetric dielectric shield, as schematically illustrated in Fig. 1(c), selectively makes one nanorod less influential to the surrounding condition. This asymmetry should substantially modify the relative phase between the scattered fields of the two nanorods and reverse the constructive and destructive interference when one resonance crosses the other, as shown in Fig. 1(d). As a result, the direction of light scattering can reverse depending on the ambient medium when asymmetric shielding is applied.

Figures 2(a) and 2(b) show the schematic illustration and scanning electron microscope (SEM) image of the plasmonic nanoantenna with the asymmetric dielectric shield. We used gold as the plasmonic nanoantenna material owing to its long-term stability and Al_2O_3 as the dielectric shield because of its high transparency of light. Our device architecture can also be applied to other plasmonic nanoantenna materials and transparent dielectric shields for a wide range of practical applications. For instance, silver offers advantages for operation in the visible spectral range. Paired gold nanorods were fabricated on a glass substrate with electron beam lithography (EBL) and metal deposition (supplementary material). We used 5-nm-chromium as an adhesion layer for gold, which may increase the optical absorption and linewidth. The optical absorption can be suppressed by employing a thinner adhesion layer. The width, height, and distance of the two nanorods were 60, 50, 350 nm, respectively, while the lengths were 130 and 110 nm, which were extracted from the SEM image without the dielectric shield (supplementary material), respectively. The distance of 350 nm induced the phase retardation of 0.78 π along the scattered angles. This retardation exceeding 0.5 π was designed to obtain high and reversible directionality of the scattered light (supplementary material). The shorter nanorods were selectively coated with amorphous Al_2O_3, whose width and height were 150 and 70 nm, respectively, with pulse laser deposition. The deposited Al_2O_3 was optically transparent in relevant wavelength range. Because the shorter nanorods were fully embedded in Al_2O_3 and the glass substrate, their resonance frequencies should be less affected by the change in the ambient refractive index, while the longer nanorods should exhibit the resonance shifts in response to the surrounding medium. To ensure sufficient scattering intensity, the nanoantennas were arranged into square arrays, as shown in Fig. 2(c). The periodicities in the x- and y-directions were 900 and 400 nm, resulting in diffraction angles of 35.8° for x-direction while the laser was not diffracted in y-direction at a wavelength of 800 nm.

We investigated the optical responses of the nanoantennas under different ambient conditions by extinction spectra taken with a micro spectroscopic system. A broadband white-light source, whose wavelength covered from 650 to 1000 nm, was focused onto the nanoantennas through an objective lens with a numerical aperture (NA) of 0.3. The transmitted light was corrected with an oil-immersion lens (NA = 1.49) and analyzed with a spectrometer. To maximize the signal to noise ratio, the incident light was linearly polarized to the nanoantennas. All extinction spectra were normalized by the reference spectra taken at the substrate regions without nanoantennas (supplementary material).

Figure 3(a) shows the extinction spectra of the nanoantennas without dielectric shields. The black curve corresponds to measurements in the air, while the red curve was obtained with a water droplet applied to the sample. Each spectrum was composed of two peaks corresponding to the resonances of the long and short nanorods. Therefore, the overall linewidth of the nanoantenna spectrum arises from the individual linewidths of each rod and the frequency separation between their resonances. The full-width-half-maximum (FWHM) of the peak taken in air and those in water were 106 and 100 nm, respectively. The water droplet increased the local refractive index, causing both resonance peaks to shift to longer wavelengths. Because the amounts of shifts were similar for both nanorods, the overall spectral linewidth almost remained across the two ambient conditions. In contrast, as shown in Fig. 3(b), in the case of shielded nanoantennas, the resonance wavelengths of the shielded nanorods remained nearly unaffected by the water droplet, whereas the resonances of the other nanorods exhibited a shift. This differential response led to a significant change in the wavelength separation between the two resonances, represented by the decrease in the overall spectral linewidth from 140 to 90 nm. It indicates that the relative phase and directionality of the scattered light from the shielded nanoantenna were drastically changed depending on the ambient medium.

The unidirectional light scattering of the nanoantennas was investigated with a linearly polarized continuous-wave Ti: sapphire laser. The laser was focused on and collected with the same objective lenses for the spectrum measurements. The angular distribution of the scattered light was imaged at the back focal plane of the collection objective using a charge-coupled device (CCD) camera. To suppress the directly transmitted laser beam, an opaque stopper was placed, blocking light with numerical aperture (NA) less than 0.3. The incident laser angle was aligned to be equally scattered along ±1st-order diffraction of the symmetric single nanorod array, which confirmed that the laser was introduced vertically on the nanoantennas (supplementary material).

Figure 3(c) shows the Fourier images of the scattered light of unshielded nanoantennas at an incident wavelength of 780 nm with and without the water droplet. Bright spots in the images

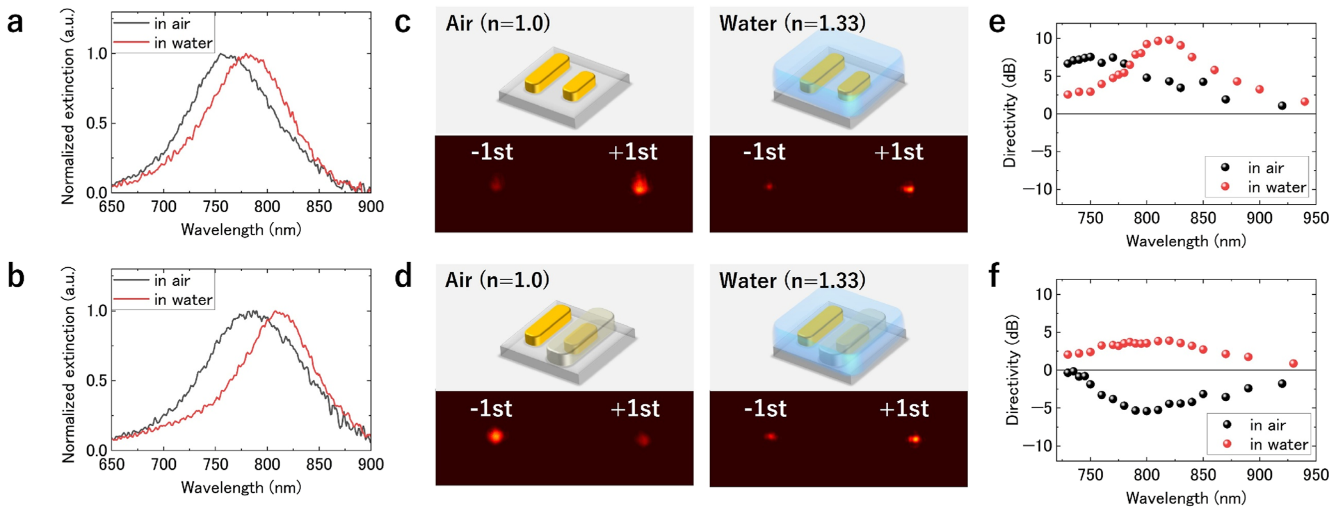

FIG. 3. Extinction spectra of the unshielded (a) and shielded (b) nanoantennas in air (black) and with water droplet (red). CCD images of the scattered light along ±1st-order diffraction of the unshielded (c) and shielded (d) arrayed nanoantennas with and without water droplets. The incident laser wavelength was 780 nm (800 nm) for the unshielded (shielded) nanoantenna. Wavelength dependence of directivity of the unshielded (e) and shielded (f) arrayed nanoantennas with and without water droplets.

correspond to the ±1st-order diffraction, determined by the periodicity of the nanoantenna array. Due to the interferences between the two nanorods, the scattered light was dominantly directed along the +1st-order diffraction. The scattering direction remained unchanged between air and water environments, indicating that the sign of the relative phase between the nanorods was preserved under both conditions. We evaluated directivity, defined as $10\log_{10}(I_{+1}/I_{-1})$ [dB], where $I_{\pm 1}$ denote the integrated intensities of the scattered light in the ± 1st-order diffraction directions. Figure 3(e) shows the wavelength dependence of the directivity for the unshielded nanoantennas. The wavelength for the maximum directivity shifted with the water droplet, which agreed with the resonance shift observed in the spectra [Fig. 3(a)]. However, the sign of the directivity did not invert over the measured spectral range. In contrast, the nanoantennas with asymmetric dielectric shields exhibited pronounced changes in scattering behavior under different ambient conditions. As shown in Fig. 3(d), the direction of the scattered light at 800 nm reversed depending on the environment. The scattering was directed along the −1st-order in the air and switched to the +1st-order in the presence of the water droplet. This reversal persisted over a broad wavelength range, as shown in Fig. 3(f), with directivity exceeding 8.0 from 780 to 830 nm. This broadband reversal, enabled by the asymmetric dielectric shielding, offers significant advantages for sensing applications and broadband optical routing.

III. DISCUSSION

We numerically investigated the optical responses and unidirectional light scattering of the fabricated nanoantenna with an asymmetric dielectric shield using the finite element method (COMSOL Multiphysics). The refractive indices of the dielectric shield, water, and air were set to 1.45, 1.33, and 1.00, respectively. Figures 4(a)–4(c) show the simulated extinction spectra, the spatial distribution of scattered light intensity in the x–z plane at a wavelength of 840 nm, and the wavelength dependence of the directivity, with and without a water droplet. We also calculated those of unshielded nanoantenna (supplementary material). The experimental results were well reproduced by these numerical simulations, verifying the validity and applicability of the numerical model. We further calculated the directivity of the nanoantennas at a laser wavelength of 840 nm with and without dielectric shields as a function of the ambient refractive index ranging from 1.00 to 1.35, as shown in Fig. 4(d). The shielded nanoantenna exhibits a broader linear response regime to the ambient refractive index compared to the unshielded nanoantenna, providing an extended dynamic range and enhanced sensitivity for sensing applications. For the shielded nanoantenna, we calculated the near-field distribution (supplementary material) and evaluated the field leakage ratio for various shield widths, defined as the field amplitude outside the shield normalized by the total field amplitude. The field leakage makes the resonance of the shielded nanorod less stable against environmental changes. To evaluate the sensitivity to local solvent volume, we simulated a gradual reduction of solvent thickness around the nanoantenna and calculated the differential directionality relative to that in air, as shown in Fig. 4(e). Owing to the strong localized optical field of the plasmonic nanoantenna, 80% of the intensity ratio was maintained even when the solvent thickness was reduced to 80 nm. These results indicate that the local molecular adsorption onto the antenna surface can be detected via directional light scattering.

Finally, let us discuss the optical recoil forces arising from unidirectional side scattering by our nanoantenna. The nanoantenna experiences a lateral optical force perpendicular to the incident light momentum and this force changes depending on the surrounding refractive index, as shown in Fig. 4(f). It should be noted that not only the magnitude but also the direction of the lateral force can be controlled according to the surrounding refractive index. The

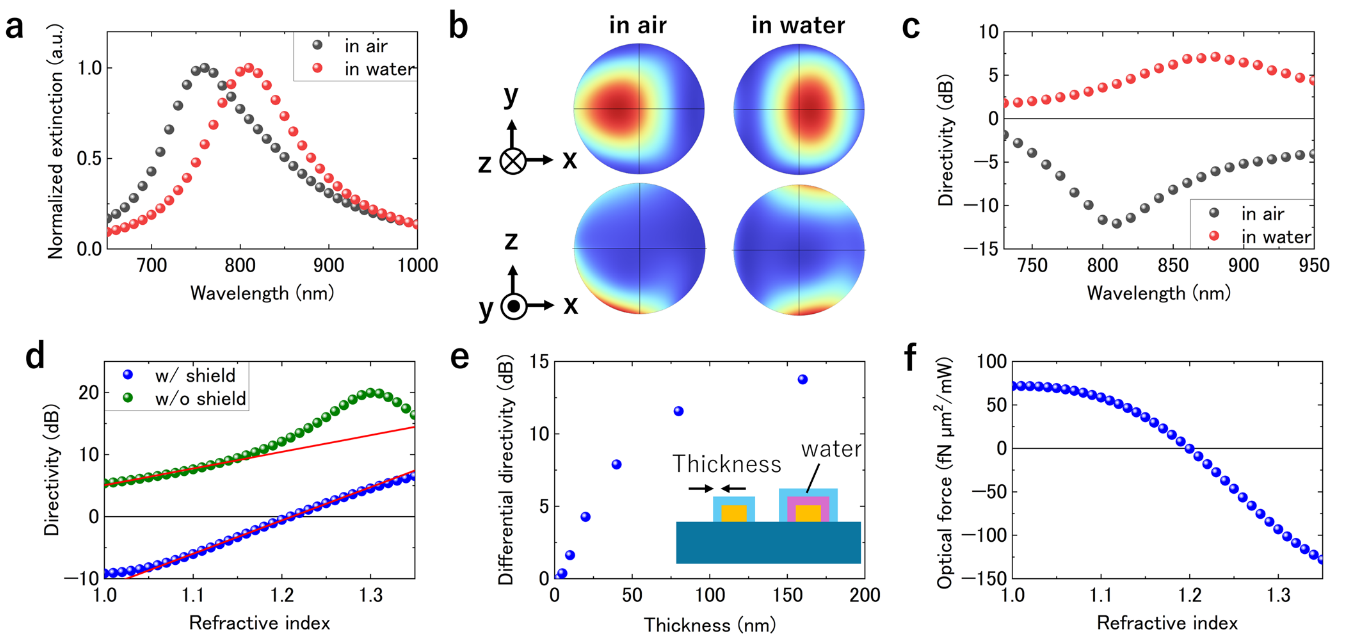

FIG. 4. (a) Numerically calculated extinction spectra. (b) Scattering intensity distributions at a wavelength of 840 nm in X–Y and X–Z planes. (c) Wavelength dependence of directivity. (d) Refractive index dependences of directivity of the nanoantenna with (blue circles) and without dielectric shield (green circles). The red lines indicate the fitted curves within the linear response regimes. (e) Differential directivity as a function of water layer thickness. The inset shows a schematic image of the simulation model. (f) Lateral optical force as a function of the surrounding refractive indices.

lateral forces exceeding ±70 fN μm^2/mW obtained in media with refractive indices of 1.0 and 1.3 are sufficient to enable operation as optical nanomotors by overcoming the Brownian motion, as discussed in Ref. 24. Therefore, if similar refractive index changes can be achieved through the molecular absorption on the antenna surface, such ambient-dependent lateral forces would pave the way for optical nanomotors capable of autonomously controlling their motion in response to environmental changes. This capability holds potential applications in microfluidic devices and microdrones for drug delivery systems.[23,33]

IV. CONCLUSION

We demonstrated robust and versatile way for ambient-dependent unidirectional light scattering using hybrid plasmonic nanoantennas composed of gold nanorods and asymmetric dielectric shields. The dielectric shields modulate the relative phase of the scattered light from the paired nanorods with respect to the surrounding refractive index, leading to control of the scattering direction and moreover reversal over a wide wavelength range, depending on the ambient conditions. The experimental results were well reproduced by numerical analyses, which indicate the potential application for molecular sensing and light-driven actuators. The use of a low-loss adhesion layer can further improve the environmental control of directivity. These results provide broadband, high-contrast, and reversible unidirectional light scattering with a compact footprint, paving the way for advanced nanophotonic sensing, integrated photonic systems, and exotic light-driven actuators.

SUPPLEMENTARY MATERIAL

The supplementary material provides the additional numerical analyses, materials, and methods including schematic images of the experimental setups.

ACKNOWLEDGMENTS

This work was supported by Grants-in-Aid for Scientific Research (KAKENHI) [Grant Nos. JP24H00424 and JP22H05132 in Transformative Research Areas (A) “Chiral materials science pioneered by the helicity of light” to Y.Y.T.] from the Japan Society for the Promotion of Science (JSPS) and the JST FOREST Program (Grant No. JPMJFR213O to Y.Y.T.). This work was supported by the JSPS Program for Forming Japan’s Peak Research Universities (J-PEAKS) Grant No. JPJS00420230001 and “Advanced Research Infrastructure for Materials and Nanotechnology in Japan (ARIM)” of the Ministry of Education, Culture, Sports, Science and Technology (MEXT). Grant No. JPMXP1225HK0011 (Hokkaido University). We thank Dr. H. Hosoi, Dr. H. Onishi, and Dr. Y. Matsuo of Hokkaido University for their helpful support in sample fabrication.

AUTHOR DECLARATIONS

Conflict of Interest

The authors have no conflicts to disclose.

Author Contributions

Shuto Watanabe: Formal analysis (equal); Investigation (lead); Resources (lead); Writing – original draft (supporting). **Ryuichi**

Ohta: Formal analysis (equal); Investigation (supporting); Project administration (equal); Resources (supporting); Writing – original draft (lead); Writing – review & editing (equal). **Tsukasa Katayama**: Resources (supporting); Writing – review & editing (supporting). **Yoshito Y. Tanaka**: Conceptualization (lead); Formal analysis (equal); Funding acquisition (lead); Investigation (supporting); Methodology (lead); Project administration (equal); Resources (supporting); Supervision (lead); Writing – review & editing (equal).

DATA AVAILABILITY

The data that support the findings of this study are available from the corresponding author upon reasonable request.

REFERENCES

[1] S. A. Maier, *Fundamentals and Appliations of Plasmonics* (Springer US, New York, 2007).

[2] T. Itoh, M. Procházka, Z.-C. Dong, W. Ji, Y. S. Yamamoto, Y. Zhang, and Y. Ozaki, "Toward a new era of SERS and TERS at the nanometer scale: From fundamentals to innovative applications," Chem. Rev. **123**, 1552 (2023).

[3] A. B. Taylor and P. Zijlstra, "Single-molecule plasmon sensing: Current status and future prospects," ACS Sens. **2**, 1103 (2017).

[4] H. Altug, S.-H. Oh, S. A. Maier, and J. Homola, "Advances and applications of nanophotonic biosensors," Nat. Nanotechnol. **17**, 5 (2022).

[5] C. Zhan, X. J. Chen, J. Yi, J. F. Li, D. Y. Wu, and Z. Q. Tian, "From plasmon-enhanced molecular spectroscopy to plasmon-mediated chemical reactions," Nat. Rev. Chem. **2**, 216 (2018).

[6] I. S. Maksymov, I. Staude, A. E. Miroshnichenko, and Y. S. Kivshar, "Optical Yagi-Uda nanoantennas," Nanophotonics **1**, 65 (2012).

[7] A. B. Evlyukhin, S. I. Bozhevolnyi, A. Pors, M. G. Nielsen, I. P. Radko, M. Willatzen, and O. Albrektsen, "Detuned electrical dipoles for plasmonic sensing," Nano Lett. **10**, 4571 (2010).

[8] T. Kosako, Y. Kadoya, and H. F. Hofmann, "Directional control of light by a nano-optical Yagi–Uda antenna," Nat. Photonics **4**, 312 (2010).

[9] D. Vercruysse, Y. Sonnefraud, N. Verellen, F. B. Fuchs, G. Di Martino, L. Lagae, V. V. Moshchalkov, S. A. Maier, and P. Van Dorpe, "Unidirectional side scattering of light by a single-element nanoantenna," Nano Lett. **13**, 3843 (2013).

[10] N. Li, Y. Lai, S. H. Lam, H. Bai, L. Shao, and J. Wang, "Directional control of light with nanoantennas," Adv. Opt. Mater. **9**, 2001081 (2021).

[11] T. Pakizeh and M. Käll, "Unidirectional ultracompact optical nanoantennas," Nano Lett. **9**, 2343 (2009).

[12] A. G. Curto, G. Volpe, T. H. Taminiau, M. P. Kreuzer, R. Quidant, and N. F. van Hulst, "Unidirectional emission of a quantum dot coupled to a nanoantenna," Science **329**, 930 (2010).

[13] H. Aouani, O. Mahboub, E. Devaux, H. Rigneault, T. W. Ebbesen, and J. Wenger, "Plasmonic antennas for directional sorting of fluorescence emission," Nano Lett. **11**, 2400 (2011).

[14] S. P. Gurunarayanan, N. Verellen, V. S. Zharinov, F. James Shirley, V. V. Moshchalkov, M. Heyns, J. Van de Vondel, I. P. Radu, and P. Van Dorpe, "Electrically driven unidirectional optical nanoantennas," Nano Lett. **17**, 7433 (2017).

[15] Y. H. Fu, A. I. Kuznetsov, A. E. Miroshnichenko, Y. F. Yu, and B. Luk'yanchuk, "Directional visible light scattering by silicon nanoparticles," Nat. Commun. **4**, 1527 (2013).

[16] M. Neugebauer, P. Woźniak, A. Bag, G. Leuchs, and P. Banzer, "Polarization-controlled directional scattering for nanoscopic position sensing," Nat. Commun. **7**, 11286 (2016).

[17] J. Du, W. Bao, R. Zhang, S. Shen, L. Yue, Q. Ding, P. Xie, X. Kuang, H. Zhang, and W. Wang, "Manipulation of unidirectional side scattering of light in transition metal dichalcogenide nanoresonators," Phys. Rev. B **109**, 115426 (2024).

[18] T. Shegai, S. Chen, V. D. Miljkovic, G. Zengin, P. Johansson, and M. Käll, "A bimetallic nanoantenna for directional colour routing," Nat. Commun. **2**, 481 (2011).

[19] Y. Y. Tanaka and T. Shimura, "Tridirectional polarization routing of light by a single triangular plasmonic nanoparticle," Nano Lett. **17**, 3165 (2017).

[20] X. Liu, A. Li, C. Liu, N. Zhao, J. Peng, F. Gan, X. Lei, R. Wang, and A. Wu, "Broadband color routing with a single element nanoantenna for communication bands," APL Photonics **9**, 076105 (2024).

[21] T. Shegai, P. Johansson, C. Langhammer, and M. Käll, "Directional scattering and hydrogen sensing by bimetallic Pd–Au nanoantennas," Nano Lett. **12**, 2464 (2012).

[22] M. Wersäll, R. Verre, M. Svedendahl, P. Johansson, M. Käll, and T. Shegai, "Directional nanoplasmonic antennas for self-referenced refractometric molecular analysis," J. Phys. Chem. C **118**, 21075 (2014).

[23] M. Liu, T. Zentgraf, Y. Liu, G. Bartal, and X. Zhang, "Light-driven nanoscale plasmonic motors," Nat. Nanotechnol. **5**, 570 (2010).

[24] Y. Y. Tanaka, P. Albella, M. Rahmani, V. Giannini, S. A. Maier, and T. Shimura, "Plasmonic linear nanomotor using lateral optical forces," Sci. Adv. **6**, eabc3726 (2020).

[25] X. Wu, R. Ehehalt, G. Razinskas, T. Feichtner, J. Qin, and B. Hecht, "Light-driven microdrones," Nat. Nanotechnol. **17**, 477 (2022).

[26] R. Guo, M. Decker, F. Setzpfandt, I. Staude, D. N. Neshev, and Y. S. Kivshar, "Plasmonic fano nanoantennas for on-chip separation of wavelength-encoded optical signals," Nano Lett. **15**, 3324 (2015).

[27] P. Albella, T. Shibanuma, and S. A. Maier, "Switchable directional scattering of electromagnetic radiation with subwavelength asymmetric silicon dimers," Sci. Rep. **5**, 18322 (2016).

[28] K. Akiyoshi, Y. Y. Tanaka, T. Ishida, T. Shimura, and T. Tatsuma, "Plasmonic–diffractive hybrid sensors based on a gold nanoprism array," ACS Appl. Nano Mater. **1**, 5994 (2018).

[29] I. Tanabe, Y. Y. Tanaka, K. Watari, W. Inami, Y. Kawata, and Y. Ozaki, "Enhanced surface plasmon resonance wavelength shifts by molecular electronic absorption in far- and deep-ultraviolet regions," Sci. Rep. **10**, 9938 (2020).

[30] N. Liu, M. L. Tang, M. Hentschel, H. Giessen, and A. P. Alivisatos, "Nanoantenna-enhanced gas sensing in a single tailored nanofocus," Nat. Mater. **10**, 631 (2011).

[31] B. Luk'yanchuk, N. I. Zheludev, S. A. Maier, N. J. Halas, P. Nordlander, H. Giessen, and C. T. Chong, "The fano resonance in plasmonic nanostructures and metamaterials," Nat. Mater. **9**, 707 (2010).

[32] W. R. Erwin and R. Bardhan, "Directional scattering and sensing with bimetallic fanocubes: A complex fano-resonant plasmonic nanostructure," J. Phys. Chem. C **120**, 29423 (2016).

[33] J. Qin, X. Wu, A. Krueger, and B. Hecht, "Light-driven plasmonic microrobot for nanoparticle manipulation," Nat. Commun. **16**, 2570 (2025).